

JANUSZ R. PIECHNA \*

## NUMERICAL ANALYSIS OF MICRO RING-ENGINE FLUID DYNAMICS

This paper presents an idea and results of 2D and 3D numerical CFD simulations of the proposed ring-engine construction dedicated for air propulsion or generation of electric power. The engine is designed as the simplest construction realizing the idea of pulsating reaction chamber utilizing a constant volume combustion principle. An atypical fuel (hydrogen peroxide) is used in the analyzed construction. The proposed ring-engine has reaction chambers forming a part of a ring periodically filled by cooling air and hydrogen peroxide vapour. The  $H_2O_2$  is decomposed in exothermic reaction increasing pressure inside the chamber of constant volume. High pressure gas contents of the reaction chambers are periodically decompressed by jet nozzles generating torque. The paper contains the description of the ring-engine idea, the schematic engine geometry and a set of data visualizing pressure, velocity, temperature and species distribution inside the engine components being results of numerical simulations.

### 1. Introduction

The development of micro-air vehicles (MAVs) generated the need to have small engines with characteristics satisfying operating requirements. One of them is efficient power generation in a longer time at steady engine rotational speed (cruising conditions) [2].

Micro-gas turbine engines [4, 5], micro-rockets [10], micro-rotary internal combustion engines [6] can be used for such purposes. Have been observed dramatic reduction of efficiency of micro devices in comparison with macro-scale counterparts. Due to that, a new engine ideas, more suitable for micro-scale, had to be considered. One of such new engine ideas are wave engines [1, 7, 8, 9, 11, 12, 13, 14, 15, 16]. The proposed ring engine

---

\* *Warsaw University of Technology, Institut of Aeronautics and Applied Mechanics; ul. Nowowiejska 24, 00-665 Warsaw, Poland; E-mail: jpie@meil.pw.edu.pl*

design belongs to that group of solutions. The ring engine construction was modified to overcome some negative features of typical wave engines, like very narrow range of operational rotational speeds [14, 15, 16].

Because the combustion processes in a micro-scale dominated by high heat losses have a different behaviour than the conventional large-scale ones, it was necessary to find a working example of such a process in micro-scale. Stability of combustion process is also fuel dependent. Due to this fact, a proper fuel has also been searched for.

Adoption of a hydrogen peroxide as a fuel in micro-scale engine was biologically-inspired by a defence mechanism of an insect – a bombardier beetle [3]. The insect produces a noxious spray by reacting small amounts of hydroquinone with hydrogen peroxide in the presence of the catalysts catalase and peroxidase in a pair of small (2 mm size) combustion chambers placed in its abdomen. This exothermic reaction produces water and heats it above the boiling point. The resulting steam is ejected to strike an enemy (see Fig. 1).

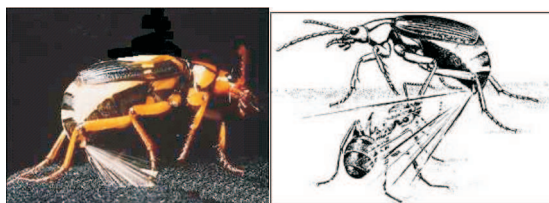


Fig. 1. Bombardier beetle in defence action – inspiration of ring engine fuel choice

The beetle does this at 400 to 500 cycles/s. Such example of successful hydrogen peroxide decomposition in micro scale ensures its repetition in technical application. Due to this fact, such an atypical fuel is used in the analyzed micro engine construction. Hydrogen peroxide has been reconsidered as a promising green fuel [2]. It also has several other unique features of the monopropellant, such as temperature control, safety, ease of use, non-toxicity and low combustion temperatures. The main advantage of the hydrogen peroxide is stability at ambient pressure in a wide range of temperatures but rapid, exothermic decomposition into water (steam) and oxygen in presence of catalyst materials such as metallic silver, manganese dioxide ( $\text{MnO}_2$ ) and dimanganese trioxide ( $\text{Mn}_2\text{O}_3$ ), or high temperature igniters [4]. This gives an easy and exact control of use of this fuel in micro scale, as well as clean and environment friendly output of hot gases.  $\text{H}_2\text{O}_2$  is stored as a liquid, requires to be heated to the saturation point (423 K) and then delivered as a vapour to the reaction chamber. At a concentration of 90%,  $\text{H}_2\text{O}_2$  is already available commercially and ensures complete decomposition at a temperature of about 1022 K. Such a temperature level of gas products of decomposition

is acceptable in silicon wafer technology, which is a great advantage of the proposed fuel.

Typically, the idea of using a catalytic bed to generate a hot stream of oxygen and steam expanded in exhaust nozzle is realized in many mono-propellant rockets [17]. Such a monopropellant like  $H_2O_2$  can be used in a simpler way in an engine utilizing principle of the Heron turbine. Propellant can be burned or decomposed in a steady-flow reaction chamber, and then delivered at high pressure to rotating nozzles generating torque. However, the proposed engine was intended to freely aspirate oxidizer and fuel, and to perform a chemical reaction in a closed volume (reaction chamber).  $H_2O_2$  is one of possible fuels to use. The mixture of oxygen and the remaining water vapour at high temperature, being the products of the hydrogen peroxide decomposition, can be combined in the reaction chamber with an additional fuel and ignited, producing hot gases under high pressure for a prime mover such as a turbine engine.

## 2. Internal combustion vs external combustion

At initial stages of a ring engine development, a three thermodynamic turbo engine cycles have been considered. Comparison between typical turbo engine cycle described by points 1-2-3-4 in T-S diagram, wave engine (points 1-2'-3'-4') and engine with pulsating combustion chamber (points 1-2'-3'') is shown in Fig. 2. Wave engine [12, 13, 14, 15, 16,] are characterised by higher operating temperatures, higher power and higher efficiency in comparison with classical turbo engine [4, 5]. Engine with pulsating combustion chamber ensures higher efficiency and relative simplicity [1].

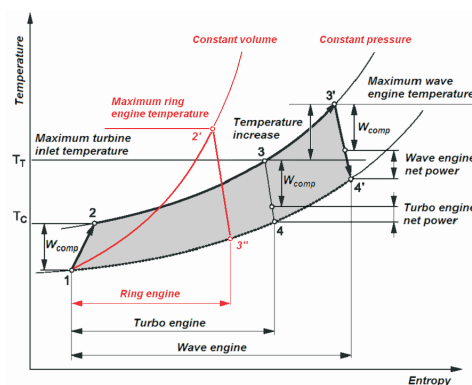


Fig. 2. Comparison of thermodynamic cycles of engines with classical combustion chamber at constant pressure with engine using pulsating combustion chamber at constant volume

The aim of the presented work was to develop the simplest engine construction demonstrating features characteristic to the engine with pulsating combustion chamber. Characteristic for that engine is combustion process realized in constant volume reaction chamber.

For the sake of simplicity in the proposed engine construction, the phase of compression 1-2 (see Fig. 2) was omitted. The proposed engine was intended to freely aspirate oxidizer and fuel and perform a chemical reaction in a closed volume (reaction chamber) starting from ambient conditions.

### 3. Fuel

The behaviour of combustion in a small scale is different from large-scale combustion phenomena mainly due to increased heat losses and reduced residence time caused by small dimensions of the device. In small-scale devices, heat loss rate is a significant factor frequently resulting in difficulties in flame stabilization and provoking flame quenching. The use of hydrogen peroxide as a fuel in micro-scale seems to be reasonable choice due to the existing biological examples confirming stable decomposition of this fuel in millimeter scale [3].

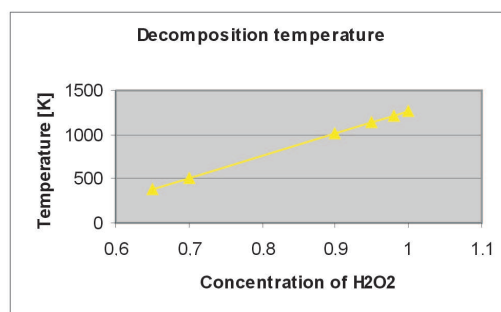


Fig. 3. Hydrogen peroxide decomposition temperature versus concentration

One of useful feature of that fuel is relatively low maximum temperature of concentration-dependent decomposition (see Fig. 3). One can see that the preferred upper temperature limit of 1000 K is easily met with 90% hydrogen peroxide. Other temperatures are easily created by blending water with hydrogen peroxide, thus producing tailored hot gas temperatures with a simple monopropellant. For concentrations over 63-64% H<sub>2</sub>O<sub>2</sub> accelerated decomposition becomes self-sustaining.

In addition, hydrogen peroxide creates a uniform hot gas source without localized hot spots or streaks of hot gas that can impinge onto turbine components [17]. Hydrogen peroxide is typically stored in liquid state inside steel container covered by Teflon layer. To be used in the ring engine, it must

be heated to (150C) 423 K and evaporated. Pressure of the fuel vapour can be controlled by adjusting the flow rate. The oxygen is one of products of the hydrogen peroxide decomposition. The free oxygen can be used to burn additional fuel in afterburner with hydrogen peroxide decomposition process as the flame stabilizer.

#### 4. Ring engine idea

Any heat engine must go through four phases of operation. The first phase is filling the reaction chamber by the fuel and oxidizer. The second phase is chemical burning of fuel accompanied by the increase of pressure. The third one is expansion of high pressure and high temperature gases generating useful work. The fourth phase consists in exhaust of the gases. First and fourth phase can be realized simultaneously.

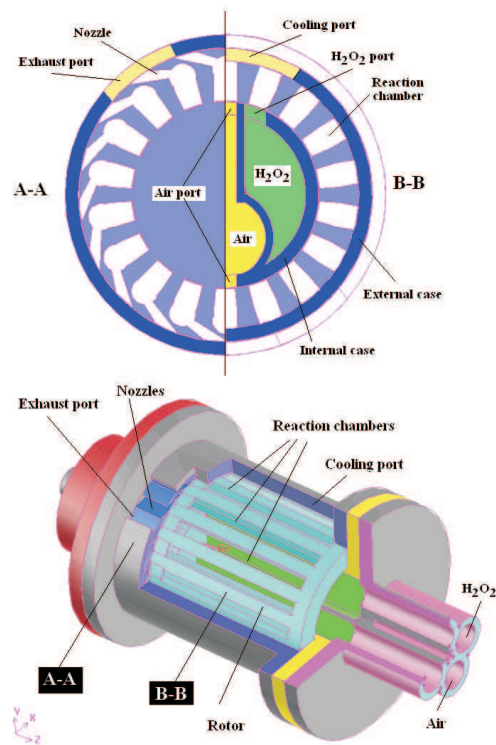


Fig. 4. Possible micro engine construction

In Fig. 4, a possible technical realization of a micro engine of 10 mm rotor diameter is presented. The set of reaction chambers constitutes the main part of the ring engine. They have the form of channels with length about 10 times longer than the channel width. In each of them, four phases of

operation must be realized sequentially. In Fig. 8, the considered phases of operation in a single reaction chamber are depicted.

The main part of the micro engine is the rotor containing walls separating reaction chambers. Internal and external sides of the chambers are closed by the cylindrical walls of the casing (see Fig. 4, Fig. 5, Fig. 6 and Fig. 7). Cooling air and fuel are delivered by slits in the internal cylindrical case. The rest of the decomposition products and cooling air are removed through the openings in the cylindrical external case. One end of each chamber is connected with periodically opened, obliquely located jet nozzles generating torque. Disk parts of the casing contain the bearings and pipes delivering cooling air and fuel.

Engine can work in a wide range of rotational speeds reaching the highest efficiency at resonant conditions. A disk version of the ring engine with radially distributed reaction chambers was also considered.

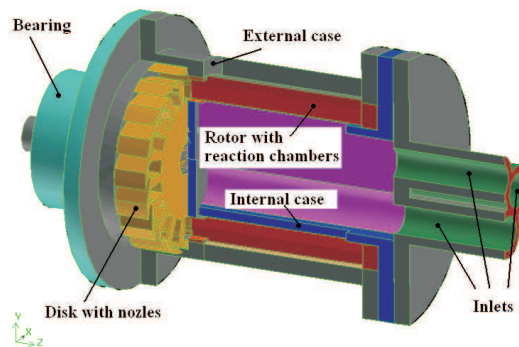


Fig. 5. Cross-section of ring engine possible technical realization

Fig. 6 shows basic engine components in an extended view.

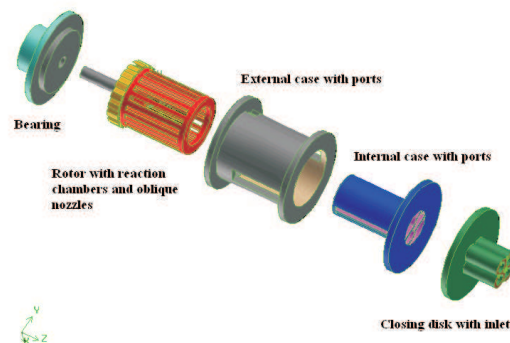


Fig. 6. Extended view of the proposed technical realization of ring engine

In Fig 7, the only rotating part of the ring engine is depicted.

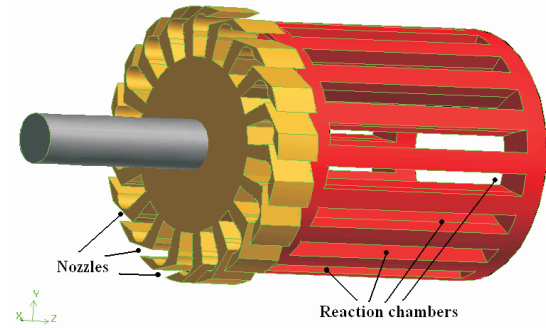


Fig. 7. Detailed view of the ring engine rotor containing a set of reaction chambers and nozzles generating torque

The single-reaction chamber, schematically presented, has three sides. The left side for inlet of cooling air and fuel, the top one containing a nozzle and the right one for outflow of exhaust gases and cooling air. These sides are periodically closed.

In the proposed ring engine construction, the idea of a sequential cross-flow has been applied. Its name reflects the principle of two main flow directions realized sequentially in the reaction chamber. The outflow of the compressed hot gases is realized along main reaction chamber axis (phase c in Fig. 8). However, the scavenging and filling the chamber by the fuel and oxidizer is realized in the direction perpendicular to the main chamber axis (phase d and a in Fig. 8). In this way, the sequential cross-flow scheme is

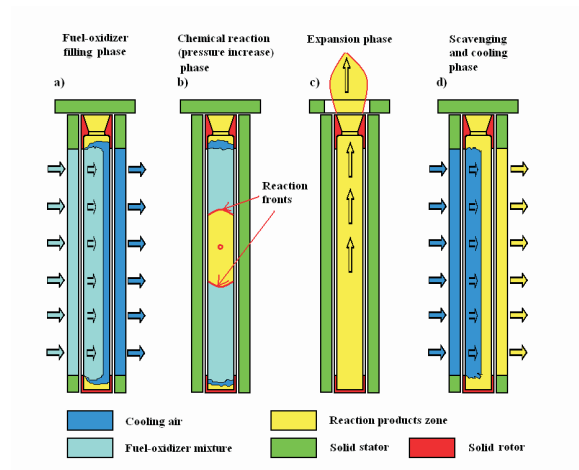


Fig. 8. Four phases of single reaction chamber operation

realized. The path of fuel motion is very short, and takes very little time even when realized with low velocity. The hot reaction chamber should be periodically cooled and fresh mixture of fuel and oxidizer should be separated by the neutral medium from the hot exhaust gas to prevent uncontrolled reaction. Because of that, the use of ambient air as a cooling and separating medium has been proposed. After expansion of hot exhaust gas, pressure in the reaction chamber drops below the ambient pressure. Such a pressure difference can be used for air aspiration. The inflow velocity in such conditions is rather low. After a while, the opposite side of the chamber can be opened and the chamber can be connected with the atmosphere (phase d in Fig. 8). The propellant mixture can be delivered at a pressure higher than the ambient one, so that the mixture delivery can be realized at a higher velocity (phase a in Fig. 8).

The operating cycle starts from the configuration shown in the sketch a) in Fig. 8. Both longer sides of the reaction chamber are opened. There is a cross flow of the mixture through the reaction chamber. When the mixture reaches the opposite chamber side (right side in Fig. 8), this side is closed. After a while also the leftover side is closed cutting off the fuel flow and totally closing the reaction chamber. Now, reaction chamber contains the mixture of the cooling air and the fuel (phase b in Fig. 8). The fuel is then ignited, or decomposition process is initiated. The burning or decomposition process progresses along its main axis by the moving fronts of reaction to the ends of the reaction chamber. The speed of reacting front propagation strongly depends on the turbulence level. After the burning (decomposition) process ends, the nozzle at one of the shorter ends opens, and the expansion process starts (phase c in Fig. 8). The reaction of the expanding gas at the nozzle generates torque. When the expansion process comes to an end, the pressure inside the reaction chamber lowers below the ambient pressure, and the longer side of the chamber (left side in Fig. 8) can be opened for cooling air delivery. A layer of neutral cold air is used for separation of fresh fuel from the hot exhausted gas (d in Fig. 8). After a while, the fuel is delivered from the left side pushing the separating air layer to the opened opposite side (a in Fig. 8). When the exhaust gas is removed from the reaction chamber, the right side of the chamber is closed. Details of this process are shown in Fig. 11 and Fig. 12.

Chemical reaction between fuel and oxidizer or decomposition of the monopropellant takes place with a limited velocity. In this specific reaction chamber geometry, the time of full decomposition of  $\text{H}_2\text{O}_2$  depends, on the one hand, on the reaction surface propagation speed, and on the other hand, on the ignition point position. To reduce the process time, ignition should be realized in the middle of the channel length. Surface propagation speed



of the reaction depends on the turbulence level, which influences the mixing process. Simple rectangular obstacles on the reaction chamber walls have been proposed as micro-vortex generators increasing the turbulence level (see Fig. 9). The expansion process (phase c in Fig. 8) is limited by the chock flow conditions at the nozzle. In general, the process time is relatively short. Due to the gas inertia, after the expansion small underpressure is generated inside the reaction chamber. The gas velocity at the nozzle is high, but in the chamber it is relatively low. Due to the high length of the reaction chamber, the processes of cleaning it from the exhaust gases and filling by the fuel/oxidizer mixture in the chamber main axis direction are rather difficult to realize and time consuming.

### 5. Numerical simulation – models

All simulations were performed by means of the FLUENT program. Flow field geometry was prepared using the preprocessor Gambit. The physical model of the compressible fluid takes into account transport of species. Four species were considered: hydrogen peroxide, oxygen, water vapour and nitrogen. The flow was treated as unsteady. Simulation of chemical reaction dynamics was based on a turbulence-chemistry interaction model. Thermal diffusion and full multicomponent diffusion was taken into account. Decomposition of  $H_2O_2$  was modelled as a single, volumetric reaction process with pre-exponential constant equal to  $1.0e13$  and activation energy of  $1.8e8$  (J/Kg/mol) [18]. The reaction of finite rate/eddy dissipation type was used with mixing rate coefficients  $A=4$  and  $B=0.5$ . Such a reaction model can be used under the assumption that turbulent flows exist, which is valid in the considered case. Both the Arrhenius rate and the mixing rate were computed and the smaller of the two was used. The turbulence relatively slowly convects and mixes cold reactants and hot products into the reaction zones, where the reaction occurs rapidly. In such cases, the combustion is limited by the mixing process. The chemical reaction rate is governed by the large-eddy mixing time scale,  $k/\varepsilon$ . Due to that, the  $k - \varepsilon$  turbulence model was applied. Because the heat loss rate is a significant factor in the development of the decomposition process, the heat exchange with walls of the reaction chamber was taken into account by application of complex wall-boundary conditions. However, any ignition source was not required to initiate combustion, but in the considered case the small area inside the reaction chamber was heated in a short time to initiate the decomposition process. Technically, ignition can be realized by a short burst of a laser beam.

Once the flame is ignited, the eddy-dissipation rate is generally smaller than the Arrhenius rate, and reactions are mixing-limited. It has been ob-

served that the reaction front propagation speed was about 10 m/s. Due to the relatively slow propagation of reaction front, the ignition area was located in the center of the reaction chamber to reduce its total time. To speed up the decomposition process in a small channel, vortex generators have been applied (see Fig. 9).

## 6. Results of 2D calculation

We have performed simulations of simplified 2D versions of a single reaction chamber with sequentially changed boundary conditions simulating all phases of operation. The decomposition process was simulated in the 2D chamber cross-section along the main axis (see Fig. 9 and Fig. 10).

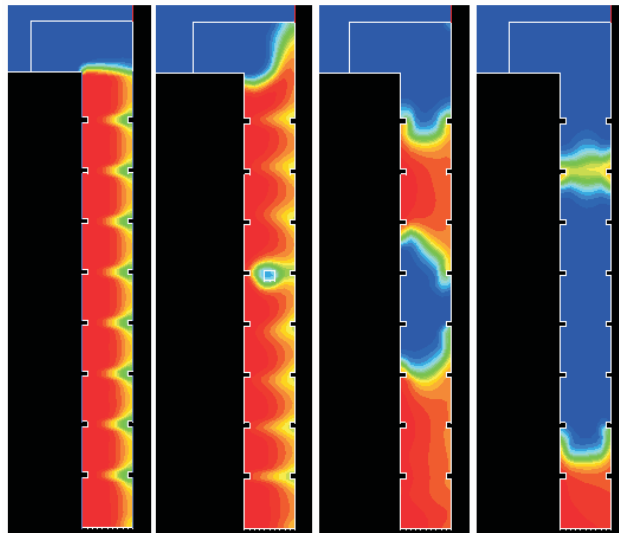


Fig. 9. Concentration of hydrogen peroxide: a) after filling process, b) just after ignition, c) during decomposition, d) just before the full decomposition (red color means high concentration, blue color low concentration)

Fig. 9 depicts the concentration of hydrogen peroxide inside the reaction chamber at different phases of cycle. Additionally, except of two reaction fronts generated by the igniter, a third front started at the contact area with the hot rest of decomposition products from the previous cycle of operation.

Three characteristic velocity patterns inside the reaction chamber are presented in Fig. 10. During decomposition phase, only local areas of the fluid motion exist near the decomposition front and in vortex generator vicinity. At the expansion phase, the highest velocity (600 m/s) exists at the nozzle and much smaller inside the chamber. During the filling phase, strong cross-flow in the chamber is generated.

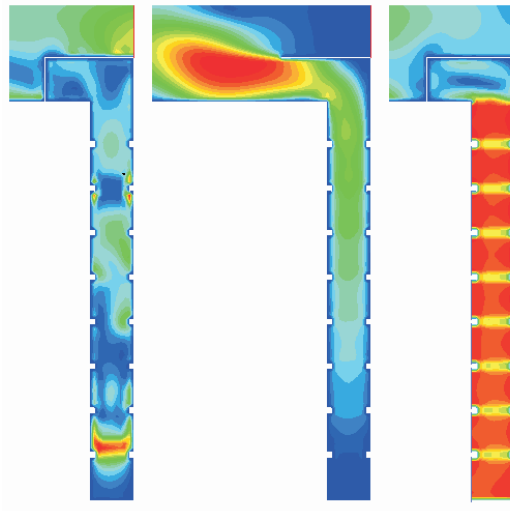


Fig. 10. Velocity magnitude distribution during decomposition phase, expansion phase and filling phase (red colour means high concentration, blue colour low concentration)

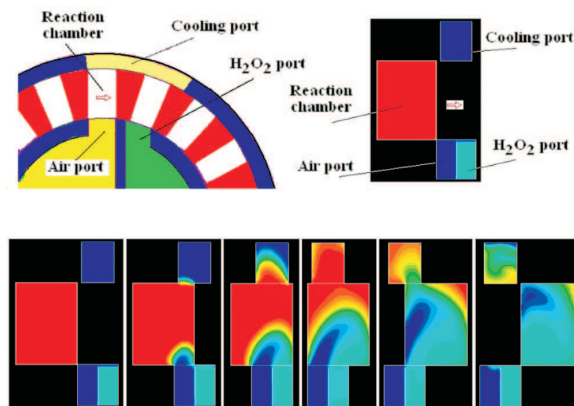


Fig. 11. Gas temperature in chamber cross-section during the cooling and filling phase (red colour means high temperature, blue colour low temperature)

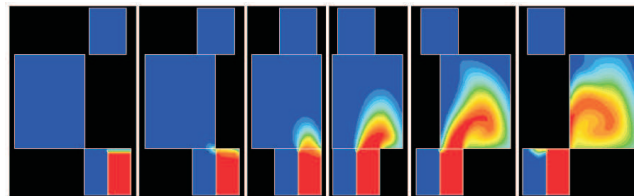


Fig. 12. Concentration of the hydrogen peroxide in chamber cross-section during the cooling and filling phase (red color means high concentration, blue color low concentration)

The process of cooling and fuel filling was analyzed in a plane perpendicular to the main axis (see Fig. 11 and Fig. 12).

The bottom left channel shown in Fig. 11 and 12 contains air at a temperature of 300 K, and the bottom right channel is filled by hydrogen peroxide at a temperature of 423 K. By comparing simultaneously frames in Fig. 11 and Fig. 12, one can analyze the process of cooling and fuel filling.

Fig. 13 shows how the pressure inside the reaction chamber builds up.

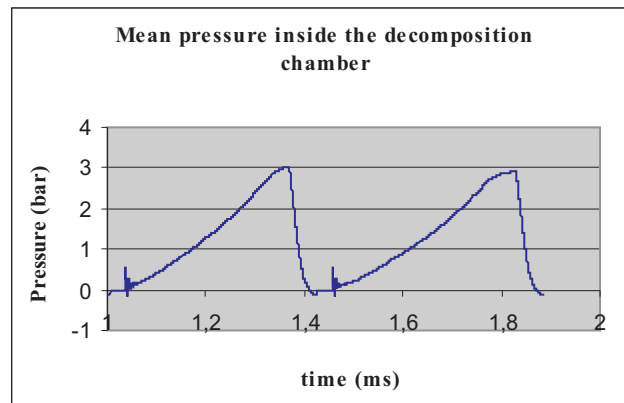


Fig. 13. Variation of the reaction chamber pressure in two cycles

The time of  $\text{H}_2\text{O}_2$  decomposition is the dominating time in the cycle. Thanks to the cross-flow idea, cooling, cleaning and filling of the reaction chamber with fuel takes only 20% of the working cycle time.

## 7. Results of 3D calculation

Following to the analysis of the results of 2D calculations, a 3D model of ring engine was developed. Because flow and thermodynamic processes in each reaction chamber are totally independent, at the beginning the scavenging, filling, decomposition and expansion processes have been simulated using the 3D model of a single chamber. The complete 3D model of moving reaction chamber, along with steady 3D models of all passages and environment area, fully represents main three-dimensional flow and thermodynamic processes during simulated ring engine operation. Main zones of the flow model are presented in Fig. 14. Red colour denotes the interfaces between the rotor and stator parts.

An instantaneous hydrogen peroxide 3D distribution inside the single reaction chamber (visualized in selected cross-sections), presented in Fig. 15, can be compared with 2D distribution shown in Fig. 9 and Fig. 12. One

can notice a strongly non-uniform distribution in longitudinal and crosswise direction.

Similar comparisons can be done for temperature distribution in 3D presented in Fig. 16 and 2D depicted in Fig. 11. It seems that the volume of the cooling air and hydrogen peroxide must be high enough to reduce the longitudinal differences of fluids delivering to the reaction chambers.

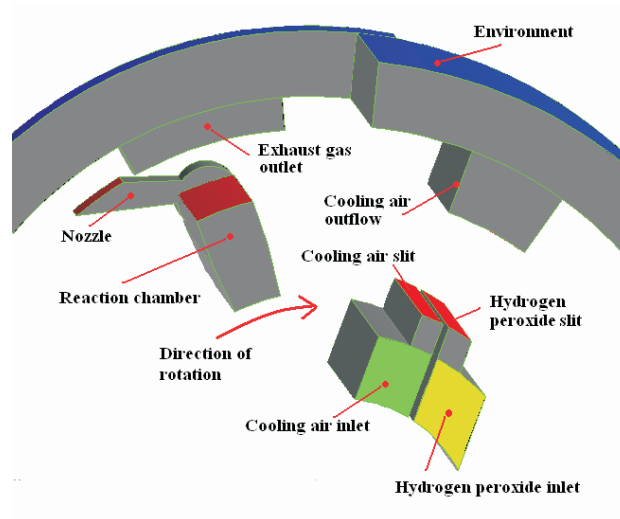


Fig. 14. Main simulated flow areas for ring engine 3D calculations (red surfaces – interfaces) – view from inlets side

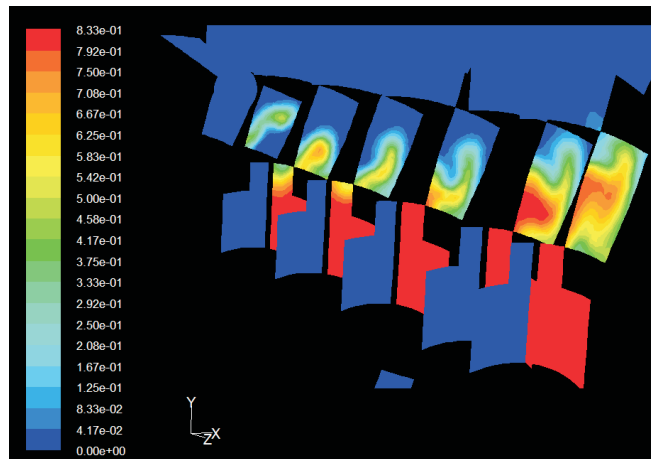


Fig. 15. Instantaneous hydrogen peroxide distribution inside single reaction chamber just after the end of the cooling and filling phase in selected chamber cross-sections

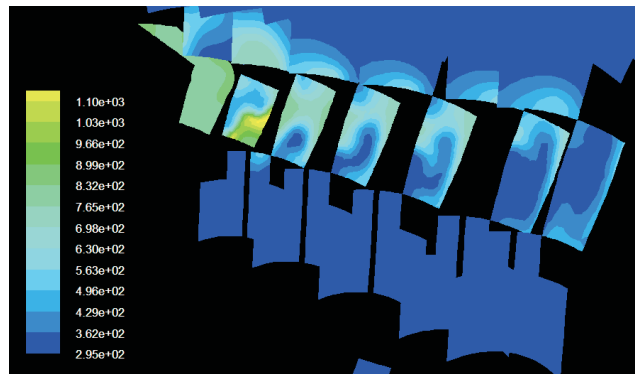


Fig. 16. Instantaneous temperature distribution inside single reaction chamber just after the end of the cooling and filling phase in a selected chamber cross-section

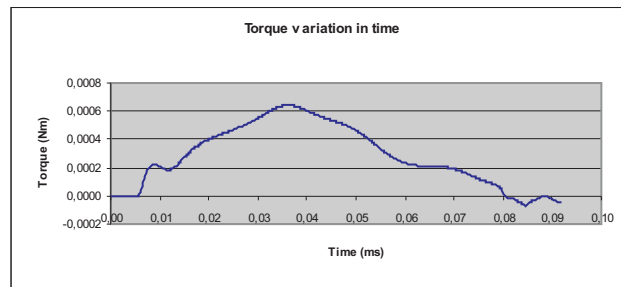


Fig. 17. Variation of the torque generated during the phase of single reaction process of chamber expansion

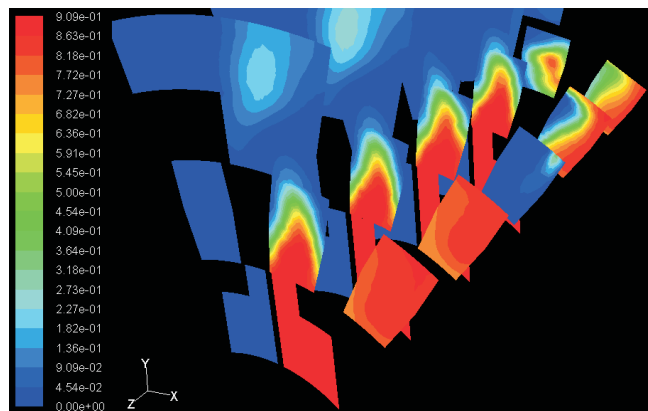


Fig. 18. Instantaneous hydrogen peroxide distribution inside three consecutive reaction chambers (before cooling, during filling and during decomposition process) in improved version of supply system in selected chamber cross-sections

The nozzles connected with reaction chambers are opened sequentially generating torque during the reaction chamber expansion phase. Fig. 17 presents variation of the torque generated by a single nozzle.

After improvement of the supply part of engine, the cooling and fuel filling process becomes axially more uniform (see Fig. 18). Low concentration of hydrogen peroxide in the central part of front chamber is the result of the decomposition process initiated at that place. To improve the scavenging process, a jet air extractor utilizing the unsteady jets generated by rotor nozzles was modelled and its operation numerically tested.

Micro-engine (10 mm rotor diameter) can generate up to 35 W of mechanical power rotating at 75 000 rpm. Maximal rotational speed is practically limited by the speed of decomposition process, which has a dominating influence (see Fig. 13).

The estimated power to volume ratio is about 10 W/cm<sup>3</sup> and power to mass ration is about 4 W/g.

### 8. From micro to macro

The analysed construction of a micro-ring engine is a rare example of solution developed for micro-scale application which can be used also in macro scale.

The proposed idea of the cross-flow developed for the use in micro scale can be realized in macro scale in a periodic combustion chamber gaining pressure and in that manner reducing the number of compressor stages required to realize the expected turbo-engine pressure ratio.

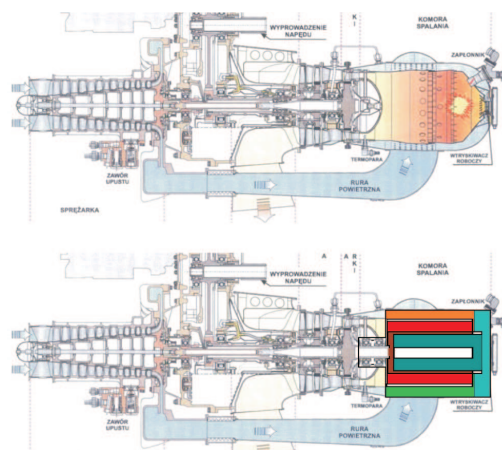


Fig. 19. Project of the helicopter turbo engine GTD 350 improved by application of pulsating combustion chamber

Typical helicopter engine GTD-350 can be improved by replacing the steady-state combustion chamber by a rotating set of reaction chambers realizing the cross-flow concept, as shown in Fig. 19.

## 9. Conclusions

Due to the observed dramatic reduction of efficiency of micro devices in comparison with macro-scale counterparts, the idea of a new engine, more suitable for micro-scale, has been considered. The proposed ring engine design belongs to wave engine type. The ring engine construction was modified to overcome very narrow range of operational rotational speeds, characteristic for conventional wave engines. The presented ring engine idea contains one breaking innovation in wave engines construction. It is the application of the cross-flow inside the combustion chamber introduced in order to reduce the times of cooling and fuel filling. In that way, the wave processes became less important and less critical than in the classic construction. The engine can work in much wider range of rotational speeds. The proposed idea of the cross-flow can be also realized in macro scale at periodic combustion chamber gaining pressure, and in that manner reducing the number of compressor stages required to realize the expected turbo engine pressure ratio. The ring engine development process, illustrated by some results of numerical calculations of operation of 2D and 3D engine models, has been shown in this paper. The results of numerical simulations confirmed the initial assumptions. A rather atypical fuel (hydrogen peroxide) was used, which was inspired by biological example of its stable decomposition in millimetre scale. Due to the existence of a free oxygen resulting from this fuel decomposition, an afterburning process can be realized by addition of conventional fuel and application of hot products of decomposition for afterburner flame stabilization.

It seems to be necessary to do simple experiments with thermal decomposition of hydrogen peroxide in micro-channels to define the real speed of reaction front and pressure and temperature increase in such conditions.

Numerical simulations of the work of ring engine with afterburner and different fuels are planned in future projects.

Manuscript received by Editorial Board, March 05, 2009;  
final version, October 05, 2009.

## REFERENCES

- [1] Akbari P., Nalim M. R., Wijeyakulasuriya S. D., Müller N.: Wave Disk Engine for Micro-Scale Power Generation, AIAA 2008-4879, 44<sup>th</sup> AIAA/ASME/SAE/ASEE Joint Propulsion Conference & Exhibit 21-23 July 2008, Hartford, CT.



- [2] Cheung W. S., Tilston J. R.: "Hydrogen Peroxide Based Propulsion System for Micro Air Vehicle Applications," ISABE-99-7278, 1999.
- [3] Eisner T., et al.: Spray Mechanism of the most primitive Bombardier Beetle (*Metrius Contractus*), *The Journal of Experimental Biology* 203, 1265-1276, 2000.
- [4] Epstein A. H.: "Millimeter-scale, MEMS gas turbine engines," GT-2003-38866, Proc of ASME Turbo Expo 2003, June 16-19, 2003, Atlanta, Georgia, USA, 2003.
- [5] Epstein A. H.: "Millimeter-Scale, Micro-Electro-Mechanical Systems Gas Turbine Engines," ASME Journal of Engineering for Gas Turbines and Power, Vol. 126, No. 2, 2005, pp. 205-226.
- [6] Fernandez-Pello A. C., Pisano A. P., Fu K., Walther D. C., Knobloch A. K., Martinez F. C., Senesky M., Stoldt C., Maboudian R. M., Sanders S., Liepmann D.: "MEMS Rotary Engine Power System," Proceedings of IEEE Transactions on Sensors and Micromachines, Vol. 123, No. 9, 2003, pp. 326-330.
- [7] Frąckowiak M., Iancu F., Potrzebowski A., Akbari P., Müller N., Piechna J.: "Numerical simulation of unsteady flow processes in wave rotors," IMECE2004-60973, 2004.
- [8] Iancu F., Piechna J., Dempsey E., Müller N.: "Ultra-Micro Wave Rotor Investigations," Technical Digest PowerMEMS 2005, The Fifth International Workshop on Micro and Nanotechnology for Power Generation and Energy Conversion Applications, Nov. 28-30, 2005 Tokyo, Japan, pp. 93-96.
- [9] Iancu F., Piechna J., Dempsey E., Müller N.: "The Ultra-micro Wave Rotor Research at Michigan State University," The 2<sup>nd</sup> International Symposium on Innovative Aerial/Space Flyer Systems (Dec. 2-3, 2005 The University of Tokio) PL-12, pp. 65-70.
- [10] London A. P., Epstein A. H., Kerrebrock J. L.: "A High Pressure Bipropellant Microrocket Engine," Journal of Propulsion and Power, Vol. 17, No. 4, 2001, pp. 780-787.
- [11] Piechna J., Akbari P., Iancu F., Müller N.: "Radial-flow wave rotor concepts, unconventional designs and applications," IMECE2004-59022, 2004.
- [12] Piechna J.: "Wave Machines, Models and Numerical Simulation", Oficyna Wydawnicza Politechniki Warszawskiej, Warszawa, 2005.
- [13] Piechna J.: "Feasibility Study of the Wave Disk Micro-Engine Operation," Technical Digest PowerMEMS 2005, The Fifth International Workshop on Micro and Nanotechnology for Power Generation and Energy Conversion Application, Nov. 28-30, 2005, The University of Tokyo, Tokyo, Japan pp. 69-72.
- [14] Piechna J.: "The micro jet wave engine idea," The 2<sup>nd</sup> International Symposium on Innovative Aerial/Space Flyer Systems (Dec. 2-3, 2005 The University of Tokio) PL-12, pp. 71-78.
- [15] Piechna J.: "Feasibility study of the wave disk micro-engine operation", Journal of Micro-mechanics and Microengineering, 16, 270-281, 2006.
- [16] Piechna J., Dyntar D.: "Two-Dimensional Numerical Analysis of the Wave Jet Micro-Engine Operation," Power MEMS2007, Freiburg Germany 2007.
- [17] Ventura M, Wernimont E, Dillard J: "Hydrogen Peroxide - Optimal for Turbomachinery and Power Applications," AIAA 2007-5537, 2007.
- [18] Sengupta D., Mazumder S., Cole J., Lowry S.: "Controlling Non-Catalytic Decomposition of High Concentration Hydrogen Peroxide," Report R3JL CFD Research Corporation 2004.

### Numeryczna analiza dynamiki przepływu w ciepłym silniku-pierścieniowym

#### Streszczenie

W pracy przedstawiono wyniki dwu i trój-wymiarowej symulacji działania proponowanego silnika pierścieniowego przeznaczonego do napędu statków powietrznych lub wytwarzania en-

---

ergii elektrycznej. Silnik charakteryzuje się najprostszą konstrukcją realizującą ideę spalania przy stałej objętości. Do jego napędu zostało użyte nietypowe paliwo jakim jest nadtlenuk wodoru. Proponowany silnik posiada komory reakcyjne rozmieszczone na obwodzie cylindra tworząc system komór okresowo napełnianych przez chłodzące powietrze i pary nadtlenuk wodoru. Paliwo to w wysokiej temperaturze ulega rozkładowi któremu towarzyszy generacja ciepła powodując wzrost ciśnienia w komorze reakcyjnej o stałej objętości. Powstające gazy o wysokim ciśnieniu po rozprężeniu wytwarzają moment obrotowy. Praca przedstawia ideę konstrukcji silnika, jego schematyczną geometrię oraz przedstawia wyniki symulacji w postaci rozkładów ciśnień, prędkości, temperatur i rozkładów składników mieszaniny gazów we wnętrzu silnika. Zaproponowano nowy sposób napełniania komory reakcyjnej paliwem skracający kilkakrotnie czas jej przepłukiwania i napełniania. Pokazano przykłady rozkładów parametrów przepływu w kilku fazach pracy silnika uzyskane z obliczeń numerycznych. Oszacowano osiągi mikro-silnika.